Asymmetric Vortex Effects on Missile Configurations

J.E. Fidler* and M.C. Bateman†
Martin Marietta Aerospace, Orlando, Fla.

An engineering procedure for estimating the effects of asymmetric lee side vortices on slender missile configurations is described. A computerized model is used which incorporates both theoretical and empirical bases. Vortex locations and strengths are defined on mainly empirical grounds. Forces and moments are calculated from potential flow considerations. The procedure may be applied to bodies with or without tails. Among the effects calculable are: induced side forces, yawing moments, tail forces, and rolling moments. Comparisons between predicted and experimental effects are shown. Procedure accuracy is generally suitable for preliminary design purposes.

Nomenclature

A = reference area
a = body radius
AR = tail aspect ratio
C_A = axial force coefficient
C_{dc} = cross-flow drag coefficient
C_L = lift coefficient
C_ℓ = rolling moment coefficient
C_N = normal force coefficient
C_n = yawing moment coefficient
C_Y = side force coefficient
d = missile body diameter
e = axial extent of base influence
F = vorticity flux
g = axial distance over which boundary layer is shed to form vortex
h = vortex street lateral dimension
K = coefficient in vortex strength equation
l = length
ℓ = vertical distance between vortices of like sign
M = Mach number
m = number of vortices in wake at a given axial location on the body
n = frequency with which vortices of like sign are shed
p = spanwise distance from tail root to tip
$\bar{R}$ = radial limit of vortex influence on a body
R_e = Reynolds number
r = radial distance from center of body
S = Strouhal number $= nd/V \sin\alpha$
U_s = circumferential velocity at edge of boundary layer at separation
V = freestream velocity
v = velocity induced normal to tail leading edge in the y direction
x = axial distance along body
Y = side force
y = lateral distance normal to body
z = distance above and normal to body axis
α = angle of attack
δ = nose half angle
σ = angle between growing vortex cores and body axis
θ_s = circumferential separation point angular orientation
ξ = angle between street vortex cores and body axis
Γ = vortex strength
$\Gamma(x)$ = local value of strength in a growing vortex
ρ = freestream density
ϕ = roll angle
χ = separation angle parameter
λ = tail taper ratio

Subscripts

a = axial direction
B = body
c = cross flow
i = induced; vortex indicator
L,R = left and right sides of body, respectively
0 = initial condition
s = vortices, starting with third from missile nose
T = tail
x = conditions at axial station x
$1,2$ = first and second vortices, respectively

Presented as Paper 75-209 at the AIAA 13th Aerospace Sciences Meeting, Pasadena, Calif., January 20-22, 1975; received February 24, 1975; revision received June 5, 1975.

Index categories: LV/M Aerodynamics; Jets, Wakes, and Viscid-Inviscid Flow Interactions; Viscous Nonboundary-Layer Flows.

*Staff engineer; Aerophysics Department. Presently a member of Engineering Management at Nielsen Engineering and Research, Mountain View, Calif.

‡Senior Engineer, Aerophysics Department.

Introduction

In recent years, increased maneuverability requirements for air-to-air missiles have dictated corresponding increases in angles of attack, particularly for those vehicles which perform slewing maneuvers. Maximum angles for such missiles can now reach 180°. As a result of these developments, the flowfields with which the aerodynamicist has to deal are much more complex, and traditional methods for predicting aerodynamic characteristics are inadequate to deal with all the problems involved. One example of method deficiency is found in the angle of attack range 25-50°. Here, steady, asymmetric vortex patterns which usually develop in the body wake, can induce large side forces and yawing and rolling moments, which are detrimental to missile controllability. Few methods are currently available for predicting these forces and moments or for analyzing the complex flowfields which produce them. The effects are particularly acute in the subsonic-transonic speed range. At Mach numbers greater than about 1.5, however, they tend to diminish rapidly.

The flow phenomena involved and their effects have received considerable attention recently,[1-9] although wake vortex effects and asymmetry have been reported by earlier authors.[10-13] Among the earliest studies were those of Allen and Perkins[10] and Perkins and Jorgensen,[11] in which some of

the basic flow structure in the wake was investigated and the onset of vortex asymmetry observed. More recent work by Thomson and Morrison[1] and Thomson[2,8] determined details of the wake flowfield and the associated vortex characteristics through direct flow probing. In that work, attention was drawn to the strong similarities between the three-dimensional asymmetric wake and its two-dimensional counterpart, the von Karman vortex street. Measurements were made of vortex strengths, spacing, and shedding frequency. The data of Ref. 1 have often formed the basis for follow-on work to determine vortex effects on slender missiles[5,8] or for the computation of wake flow charateristics.[6] The measurements form part of the basis for the present work, with suitable modifications for various flow parameter changes.

Recent wind tunnel investigations performed by Martin Marietta showed marked evidence of asymmetric vortex effects. The magnitudes of typical induced quantities are shown in Figs. 1 and 2. In Fig. 1., pitch and yaw plane moment data up to 60° angle of attack are shown for an isolated body composed of an ogive/cylinder of 10:1 total slenderness ratio. Beginning around 25° angle of attack, considerable yawing moments were induced due to asymmetries. The addition of tails to the body (Fig. 2) results in the generation of yawing moments which are almost as large as the pitching moments. In addition to the problem of magnitudes is that of unpredictable sign.[1,3,4] Random changes in direction of forces and moments have been observed, sometimes related to changing flow conditions, but often interpreted to be caused by small manufacturing imperfections near the missile nose.[1,3,4] In fact, significant changes in induced force and moment magnitudes and signs can be produced by rotation of all or parts of the body.[1,3,4] This has further, serious implications for missile controllability.

It is clear that techniques are required for calculating the forces and moments induced by asymmetric vortex wakes. Some work has already been done in this area[8,9] for slender bodies at subcritical crossflow Reynolds number. The present work deals with that case, also, but goes further in considering supercritical cross-flow Reynolds and Mach number effects for bodies with and without tails. The technique to be described is semi-empirical, drawing upon the experimental evidence referred to above, but modifying it for different flow conditions and supplementing it with analytical results and techniques. The work is confined to steady-state flow conditions. The procedure has been programmed for digital computation. Descriptions of the various bases and procedures used are given, and program predictions are compared with experimental data. It is shown that the technique provides preliminary design level accuracy for the calculation of these vortex-induced effects.

Flowfield Description

When a slender missile body is placed at angle of attack in a uniform flow, the boundary layer generally separates on either side of the body and forms a lee side wake. Separation usually begins near the rear when the missile reaches about 6° angle of attack. The wake takes the form of a pair of symmetrically disposed, counter-rotating vortices fed by vorticity shed from the separating boundary layer. As angle of attack increases, the axial extents, sizes, and strengths of the vortices increase also.

In general, vortex size and strength also increase toward the rear of the body. Several authors have formulated descriptions of vortex development along slender bodies in terms of two-dimensional, impulsively started flows around cylinders. These formulations relate flow development with time, measured either from the beginning of impulsive two-dimensional motion or from the instant a fluid particle makes contact with a three-dimensional body. In the latter case, time is defined by distance traveled along the body and the axial component of freestream velocity. For the two-dimensional case, the motion of the vortex cores as time passes (i.e., vortex size and strength increase) theoretically follows a path known as the Föppl line.[14] Use has been made of this result in the present work, as will be described later.

When the body angle of attack reaches about 25°, the symmetric nature of the wake disappears. The two vortices are joined by a third, beginning again at the body rear, and the wake becomes asymmetric. As angle is increased further, more vortices join the flow until the wake contains several which have been shed from the body. An idealized model of the flowfield is shown in Fig. 3. A section taken through the wake shows it to resemble the von Karman vortex street, well known in the literature on 2-dimensional flows. Not all of the vortices are fully shed, however; two usually remain close to the body, receiving vorticity from the shedding boundary layers. If angle of attack continues to increase, these too will be fully shed into the wake when their strength reaches some critical value. Their places will be taken by yet other growing vortices.

While a growing vortex is receiving vorticity from the boundary layer, i.e., before it reaches full strength, it tends to stay close to the body. Thomson and Morrison[1] showed schlieren photographs which implied that the vortex core is somewhat curved while it is forming. Not until full strength has been reached does the core become straight and parallel to the rest of the vortices in the street. This core behavior is indicated in Fig. 3.

It has been determined that a marked similarity exists between the manifestations and effects of two- and three-dimensional asymmetric vortex wakes.[1] In fact, the von Kar-

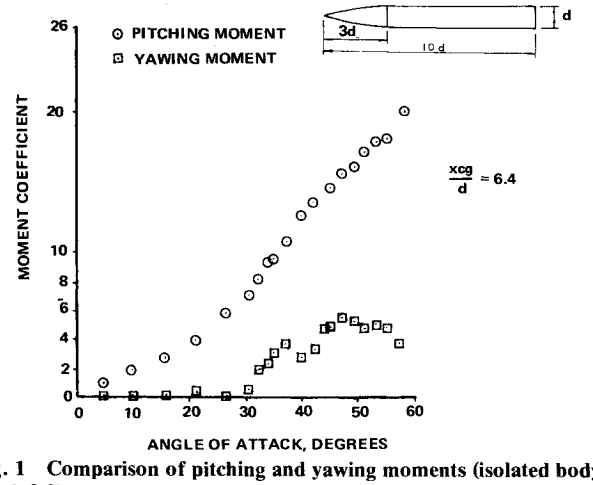

Fig. 1 Comparison of pitching and yawing moments (isolated body, Mach 0.8)

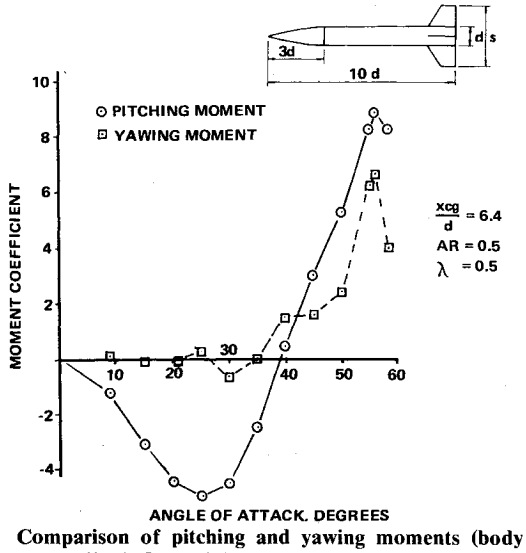

Fig. 2 Comparison of pitching and yawing moments (body with cruciform "plus" tail, Mach 0.8).

man street stability criterion that the ratio of lateral street dimension (h) to the distance between vortices of like sign (ℓ) is given by $h=0.281\,\ell$, has been shown to apply to both cases (Fig. 3). However, in the wake of Fig. 3 no lateral motion of the vortex cores relative to the body takes place. The two-dimensional phenomenon of increasing distance between vortex core and body as time increases is analogized in the same way as for the symmetrical vortices. That is to say, the wake is steady and the motion of a fluid particle along a (stationary) vortex core may again be described in equivalent time by its axial velocity and distance traveled. Through use of this analogy, Thomson[2] and Thomson and Morrison[1] were able to deduce the strengths of asymmetric wake vortices as well as their effects upon body cross-flow drag. Thomson[8] recently extended this work to deal with induced side forces and yawing moments on bodies at subcritical cross-flow Reynolds numbers.

At still higher angles of attack, say greater than 50°, the wake begins to display unsteadiness. The vortex cores show definite lateral displacements relative to the body and the induced forces and moments become time-dependent. This case will not be considered here. Consideration will be given only to the phenomena in the angle range 25-50° and their effects upon missile aerodynamic characteristics.

The first task to be performed is that of constructing a realistic flowfield model. This has been done semi-empirically based upon experimental data[1,2,8,16] and theoretical results.[14,15] Model construction is described in the next section.

Construction of Flowfield Model

The flowfield model has been constructed to reflect the aerodynamic state-of-the-art, including potential flow theory plus several of the findings of Ref. 1. Vortex strengths and locations have been made compatible with that work and suitably scaled to broaden their ranges of applicability. In addition,theoretical results on the locations of wake vortices and their images have been introduced and the contribution of nose potential lift to vortex strength has been considered. Both shed and growing vortices are treated, making use in part, of a vorticity-conservation concept.[6] Each of the above components of the model is described in detail beginning with vortex strength.

Vortex Strength

Detailed flow surveys have shown[1,8] that not all the wake vortices are of the same strength. Generally, the first vortex from the nose originates near the nose/body junction and has the smallest strength in the wake, Γ_1, say. The second vortex separates soon after the first and has a somewhat higher strength, Γ_2. From the third vortex onwards, all have approximately the same strength, $\Gamma_s\,(>\Gamma_2)$, and their spacing and strength are analogous to those of the vortices in a von Karman street. While the first and second vortex strengths will contain contributions from the (potential) nose lift, the "street" vortices are wholly fed with vorticity from the separating body boundary layer. Reference 8 presents detailed information on dimensionless vortex strength Γ_s for various angles of attack at subcritical cross-flow Reynolds number. For the first two vortices, strength is calculated using concepts from potential flow theory.

Now the first and second vortex strengths must contain a contribution from the potential flow lift of the nose. The strength of the first vortex, Γ_1, may be estimated if it is assumed that the nose is replaced by a horizontal lifting line of constant strength (Γ_1), located at the nose/body junction (Fig. 4). All of the nose lift is assumed to be generated by this line, and the associated trailing vortices will have its strength, provided they receive no further vorticity from the shedding boundary layer. The first vortex shed, near the nose body/junction, will probably contain only potential- flow-generated circulation. To calculate vortex strength, Γ_1, is straightforward. It can be shown[15] that the coefficients of normal and axial force acting on the nose are predicted by slender body theory to be

$$C_N=2\sin\alpha \qquad C_A=C_{A0}-\sin^2\alpha$$

where the reference area is that of the body cross section. Converting these quantities to lift coefficient yields

$$C_L=C_N\cos\alpha-C_A\sin\alpha$$

If C_{A0} is assumed negligible (as it will be, compared to the axial forces generated at the high angles of attack here) this expression becomes after some manipulation

$$L=(\rho/8)\,V^2\pi d^2\,(2\sin\alpha\cos\alpha+\sin^3\alpha)$$

$$=\rho\Gamma_1 dV$$

The latter expression is the well-known Kutta-Joukowski theorem. Finally, the equation may be rearranged to yield

$$\Gamma_1/Vd\sin\alpha=(\pi/8)\,(2\cos\alpha+\sin^2\alpha) \qquad (1)$$

This dimensionless vortex strength may be compared with measurements from flowfield surveys.[1] Using an angle of 30°, Eq. (1) yields a dimensionless strength of 0.78. The corresponding measured strengths from Ref. 1 show a range of values from 0.3 to 1.1, with a mean value of 0.7. This compares quite well with the predicted value. Where it is found that the first vortex is shed forward of the nose/body junction, its strength is simply determined by using the local nose diameter in Eq. (1).

There should be little or no effect of Reynolds number on Γ_1 since the strength is determined by potential flow considerations. On the other hand, Γ_s is wholly produced by viscous flow and is strongly affected by crossflow Reynolds number (R_{e_c}), which influences the characteristics of the boundary layer shed to form the street vortices. The second vortex, being shed downstream from the nose/body junction,

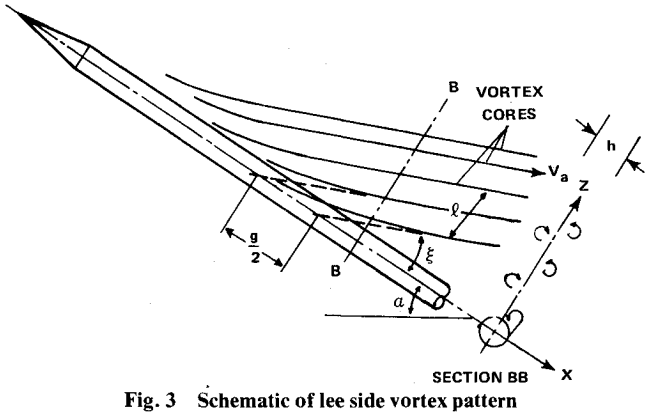

Fig. 3 Schematic of lee side vortex pattern

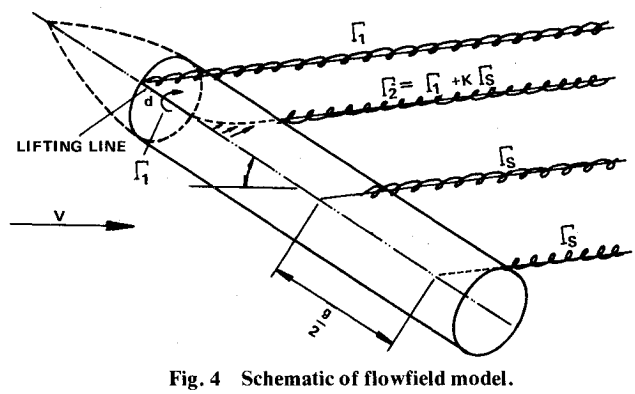

Fig. 4 Schematic of flowfield model.

is modeled here as a "mixed vortex," i.e., a potential flow vortex which receives additional vorticity from the shedding boundary layer just aft of the nose (Fig. 4). Formally, Γ_2 is expressed as $\Gamma_2 = \Gamma_1 + K\Gamma_s$. K was found empirically to be about 0.22 from the wake survey data of Ref. 1.

For street vortex strength at subcritical R_{ec}, the data shown in Fig. 5 were used.[8] To scale Γ_s for supercritical R_{ec}, use was made of von Karman's result[14] that cross-flow drag coefficient (C_{dc}) is approximately proportional to the street vortex strength, Γ_s (the expression for C_{dc} contains terms in Γ_s and Γ_s^2; however, the latter accounts for less than 10% of the total; hence, C_{dc} is approximately proportional to Γ_s). Data obtained from Martin Marietta investigations into cross-flow drag[16] produced the information of Fig. 6, which shows that for low cross-flow Mach number, cross-flow Reynolds number has a strong influence on cross-flow drag. Above the critical cross-flow Reynolds number (about 10^5), C_{dc} shows a significant decrease below the subcritical value. Hence, Γ_s, too, will be significantly reduced. An increase in cross-flow Mach number (M_c) is required to increase both C_{dc} and Γ_s. Accordingly, for $R_{ec} > 10^5$ the subcritical R_{ec} values of Γ_s from Fig. 5 are scaled in the same ratio as C_{dc} from Fig. 6.

To illuminate further the mechanisms underlying the relationship between cross-flow Reynolds number and vortex strength, recent work by Fidler[6] will be briefly described. It may be shown that the strength of a lee side asymmetric vortex can be related to the flux of cross-flow vorticity leaving the body at the circumferential separation point defined by θ_s. Further, the vorticity flux shed over axial distance g (at fixed angle of attack) in unit time is

$$F_B = \text{const} \int_0^g U_s^2 \, dx$$

The vorticity thus shed diffuses through the vortex to produce the circulation Γ_s. Equating the flux F_B to that flowing along a wake vortex of core velocity V_a yields an expression for vortex strength

$$\Gamma_s = \frac{\text{const}}{V_a} \int_0^g U_s^2 \, dx$$

Now U_s, the circumferential velocity at the boundary-layer edge at separation, is a function of θ_s. In the two-dimensional case[17] it has been found experimentally that when cross-flow Reynolds number is subcritical, θ_s lies near the meridian of the cylinder and the associated separation velocity (U_s) is larger than in the supercritical Reynolds number case, where the separation point lies far over on the cylinder lee side. Continuing the analogy between two- and three-dimensions indicates that cross-flow Reynolds number affects Γ_s through its effects; first upon θ_s, which in turn determines U_s, which defines the vorticity flux flowing from the body, and diffuses through the vortex to produce Γ_s. Hence, subcritical R_{ec} produces larger Γ values than does supercritical R_{ec}, provided cross-flow Mach number is low.

The foregoing discussions deal with fully developed vortices which have left the immediate vicinity of the body and joined the asymmetric wake pattern. However, consideration must be given to the street vortices while they are forming close to the body. As previously discussed, these growing vortices are fed by vorticity from the separating body boundary layer. Assuming rapid diffusion of vorticity, the local vortex strength $\Gamma(x)$ formed by shedding a boundary layer over distance x may be written (see previous equation).

$$\Gamma(x) = \text{const} \int_0^x U_s^2 \, dx$$

Furthermore, it has been experimentally determined[4] that, for those portions of the body where street vortices are being formed and for given flow conditions, the circumferential

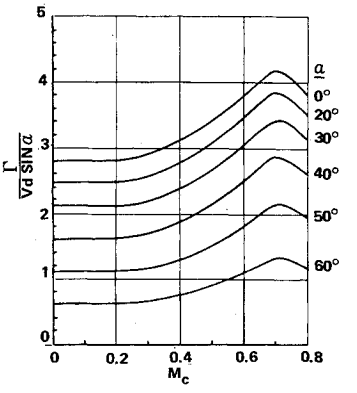

Fig. 5 Street vortex strength parameter (subcritical cross-flow Reynolds number).

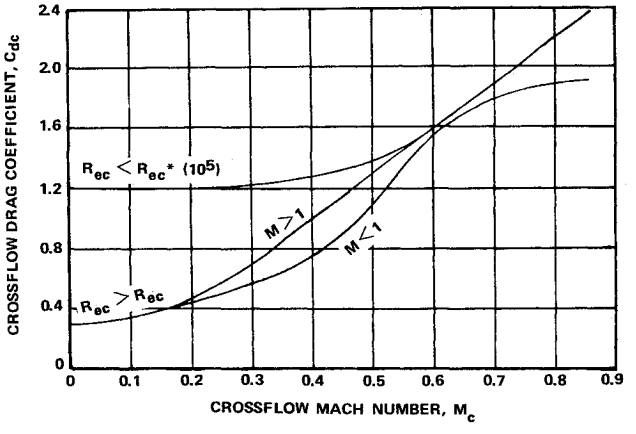

Fig. 6 Basic cross-flow drag curves for Γ_s scaling.

location of boundary-layer separation (θ_s) is approximately constant with x. Hence U_s the circumferential velocity at the boundary-layer edge at separation is also constant. Thus the local vortex strength is seen to be directly proportional to x, i.e., $\Gamma(x) = \Gamma_s \, x/g$ where g is the distance over which boundary-layer fluid is shed to form a street vortex.

One final item affecting the strengths of forming vortices has been considered. It has been shown by Thomson[8] that, as a growing vortex nears the base of the body, the rate at which its strength increases is reduced, due to base proximity. Thomson's data indicate that the growth rate is only 40% of normal. The axial extent of the region over which the base influence is felt is given by $e = d^2/2S\ell \tan\alpha$. The model contains this feature.

At any body axial station, then, the strengths of all the vortices are calculable from the combined theoretical/empirical procedures described above. The next stage in flowfield model construction is to locate the vortices relative to the body so that their effects may be calculated.

Vortex Location and Spacing

The problem of locating vortex cores in space relative to the body must be handled separately for vortices growing near the body (i.e., those being fed with vorticity from the separating boundary layer) and for shed vortices which can be considered part of the wake street. In the former case, use is made of theoretical results from two-dimensional potential flow theory; in the latter, systematic experimental evidence, suitably scaled for flow parameter changes, is employed. The case of growing vortices will be described first.

Growing Vortices

In order to model the trajectory followed by a growing vortex, two reference points are required. The first is the cir-

cumferential location on the body at which the boundary layer separates. The second is the point in space at which the vortex has reached full strength and can be said to have joined the street.

The first point is located by the empirical relationship $\theta_s = \sin^{-1}(3 \tan \delta/2 \tan \alpha)$. The angle thus defined places separation in the general region typical of laminar/turbulent boundary layers. Since the means of determining vortex strength does not rely upon an exact knowledge of the separation point location, the above approximation is sufficient for present purposes. If the determination of vortex strength had required use of the Kutta condition, or some estimate of vorticity flux leaving the body, the angle θ_s would have been required with some accuracy. In the present method however, vortex strength is defined otherwise and a rough estimate of the separation angle is sufficient.

The second point for anchoring the growing vortex trajectories was taken as the intersection of the Föppl and von Karman lines along which the symmetric and asymmetric vortex cores were known to move respectively. Use of this point was justified as follows.

As discussed earlier, the appearance of vortices in the wake shows, at the earliest stage, a symmetric pair. At any axial station, increasing angle of attack produces increased vortex size and strength as well as an outward movement of the core approximately following the Föppl line. It was reasoned that, at the first appearance of asymmetry, one of the vortices on the Föppl line would change its trajectory and proceed outwards along a new path defined by the von Karman stability relationship described earlier. The second vortex would perform similarly and this would then set up the spacing of vortices in the street. It was hypothesized, then, that in order to continue the spacing pattern, the intersection of the Föppl and von Karman lines would denote the point at which all vortices reached full strength and were shed into the street. To test this hypothesis, the schlieren photographs of Thomson and Morrision[1] were examined to determine the distance from the body where vortex feeding from the boundary layer ceased, i.e., the point at which the growing vortex cores became straight and joined the street (see earlier). It was found that the points thus defined covered a band of values from 2 to 2.5 diameters above the body and at a lateral distance defined by the von Karman stability criterion. To determine the theoretical location of the shedding point, the following procedure was used. With the equation,[14] $2ry = r^2 - a^2$, the Föppl line was drawn relative to the cylinder of Fig. 7. The data of Ref. 1 were used in the equation $d/\ell = S/\chi$ to determine ℓ, the spacing between street vortices of like sign for subcritical cross-flow Reynolds numbers. Then the von Karman relation $h = 0.281\,\ell$ was used to superimpose the street vortex location line on Fig. 7. The intersection of the Föppl and von Karman lines was found to lie within the experimentally determined range given above. It was concluded then, that this intersection point provided a good estimate of the location at which the vortices stopped growing and were shed to form part of the street. For the purposes of this engineering flow model the growing vortex core was assumed to move linearly between the two anchor points. The resulting core trajectory model is shown (foreshortened) in Fig. 8.

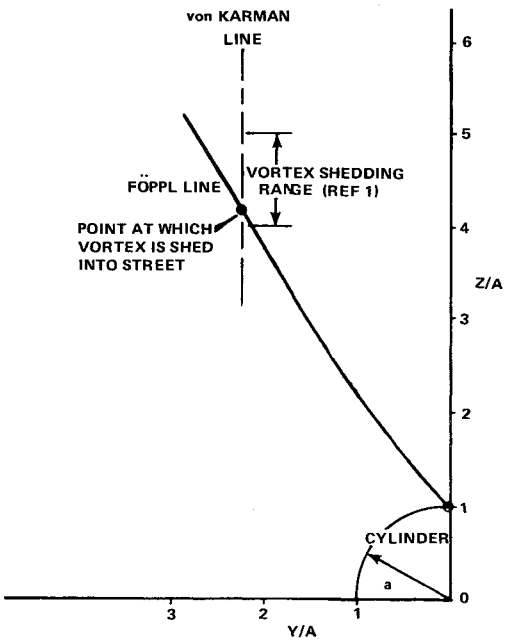

Fig. 7 Comparison between predicted and experimental point where vortex is shed into street.

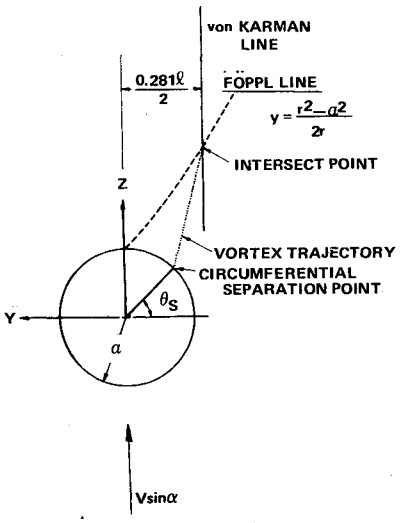

Fig. 8 Growing vortex's trajectory.

Street Vortices

From the Föppl/von Karman line intersection the vortex cores stream back into the wake as straight lines, making angle ξ with the body axis. This angle was measured by Thomson and Morrision,[1] related to the rate at which a fluid particle flowing along the core increases its distance from the body, and thence analogized to the two-dimensional von Karman street. ξ is related to missile angle of attack through the parameter $\chi = \tan \xi / \tan \alpha$ (Ref. 1). If the point on the body from which a vortex emanates is known, then its core location in space may be partly determined using χ. For the purposes of this work χ was assumed unaffected by changes in cross-flow Reynolds number.

Vortex starting points on the body were estimated in Ref. 1 as being the intersection point of the body axis and the extrapolated street vortex cores. Since these positions were obtained for tailless bodies, the present work assumes that, in the presence of tails, body vortex formation ceases at the body/tail leading edge intersection. Provided the Strouhal number (S) is known, the starting points of wake vortices can be determined. Further, using the relation[1] $d/\ell = S/\chi$, the lateral spacing (ℓ) between vortices of like sign, and hence $0.281\,\ell$, the von Karman-deduced criterion for lateral spacing can be determined. The vortex cores can now be located in space relative to the body at any point along their lengths. At this stage, however, the information is sufficient only for subcritical cross-flow Reynolds numbers.

The quantity on which attention must be concentrated when scaling vortex locations for cross-flow Reynolds number is the Strouhal number (S). This measure of the rate at which vortices of like sign are shed from the body has been shown to exhibit strong similarities between the two- and three-dimensional cases. In Ref. 1, S was determined experimentally to have values near 0.2 for a wide range of cross-flow Mach numbers. This compares well with the 2-dimensional value at

subcritical cross-flow Reynolds number. It is known, however,[8] that, for cylinders, S varies with cross-flow Reynolds number and increases to values in the range 0.3-0.5 at supercritical R_{e_c}. This has a direct effect on vortex spacing, both longitudinal and lateral. For bodies alone then, $S=0.2$ is used for subcritical R_{e_c}. It has been found that a value of $S=0.35$ gives the best results for supercritical R_{e_c}. For bodies with tails, the rate of vortex formation is influenced by the presence of the tails. Experimental evidence indicates that the effect is to reduce the rate of formation to that defined by $S=0.2$ regardless of whether the cross-flow Reynolds number is subcritical or supercritical. Accordingly, for bodies with tails, $S=0.2$ is used throughout.

At this stage, then, the strengths, numbers, and locations of the vortices on the body lee side are available, suitably scaled for the effects of cross-flow Mach and Reynolds numbers. Both growing and shed vortices have been considered and the place of experimental and theoretical inputs to their models described. The next stage is to consider their effects on the missile. This will be done separately for bodies alone and then for bodies with tails in the next section.

Force and Moment Calculations

The basic approach to calculation of the induced forces and moments involved integration of incremental effects on the bodies and tails. In order to preserve the tangency condition on the body at each axial station, image vortices are introduced. This raises a problem because of the inclination of the vortex cores relative to the body axis. A cross section normal to the street cores shows an elliptical body section, inside of which the location of image vortices is not simply accomplished. In keeping with the simple nature of this model, it was decided that, if possible, image vortices should be located by means of the circle theorem.[14] This was accomplished by resolving the vortex circulation vectors normal and parallel to the body axis. By ignoring the former as having no relevance in the two-dimensional section model, the latter components plus their images could then be used to determine forces and moments. The use of images was not necessary for body quantities; but was, however, mandatory for tailed regions of the missiles. These points are discussed below.

Body Forces and Moments

The calculation of body forces and moments begins with the determination of the incremental force on each body segment. In order to calculate this force, the local net circulation of all the vortices in the wake must be known. Further, these vortices must have their circulation vectors resolved parallel to the body, as described above. At any axial station from the nose, there are usually several wake vortices of strength Γ_s and two growing vortices, one on the left side, having strength $\Gamma_L(x)$ and another on the right, of strength $\Gamma_R(x)$. Since g is the axial distance over which a vortex grows to full strength, then $x_R=x_L+g/2$, assuming $\Gamma_R>\Gamma_L$. To resolve the strengths parallel to the body axis, the angle σ for growing and the angle ξ for street vortices were used, respectively. Side force on unit length of the body was calculated using the Kutta-Joukowski expression

$$\delta Y=\rho V\sin\alpha\left[\{\Gamma_R(x)-\Gamma_L(x)\}\cos\sigma + \left\{\sum_{i=1}^{m}\left(\frac{\bar{R}-r_i}{\bar{R}}\right)\Gamma_{sR_i}-\sum_{i=1}^{m+1}\left(\frac{\bar{R}-r_i}{\bar{R}}\right)\Gamma_{sL_i}\right\}\cos\xi\right] \quad (2)$$

where it has been assumed, for illustration, that there are $(m+1)$ fully developed vortices on the left side of the body and m on the right. The term $(\bar{R}-r_i)/\bar{R}$ is an empirical factor accounting for the attenuation of fully developed vortex effects on the body as their distances from it increases. r_i is the actual distance of the vortex from the body, and $\bar{R}$ is an arbitrary distance at which vortex effect is assumed to have attenuated to zero. The smallest value of r_i is defined by the Föppl/von Karman intersection point. This formulation was an attempt to model the expected vortex attenuation effect empirically. As will be shown later, it was found that the best representation of forces and moments was obtained when the street vortex strength was allowed to attenuate to zero immediately after shedding. Total side force Y and yawing moment YM were calculated by numerically integrating along the body length.

Tail Forces and Moments

Induced side forces, yawing moments, and rolling moments due to the presence of tails can arise even when no asymmetry exists in the wake vortex pattern. This is because of varying net angles of attack of the various tails when the missile is rolled at arbitrary angles. Hence, in order to be certain that experimental data indicate the presence of vortex asymmetry, it is necessary to be selective in choosing missile roll attitudes. For a cruciform missile, roll angles of 0 "plus" and 45° "cross" are the only attitudes where, in the absence of wake asymmetry, zero side forces, rolling moments, and yawing moments occur (assuming, of course, no tail deflections). The present model has been compared against experimental data from cruciform missiles and hence the above two roll angles will be referred to exclusively.

The procedure for calculating induced tail forces will be described for a vertical lee-side tail such as could be used on a cruciform missile in "plus" attitude. The major elements of the treatment are most expeditiously described for this case, although the complete procedure will handle tails at any roll angle so that the program can treat bodies at arbitrary roll or whose tails number other than four.

The first step in the process is to determine, for each vortex, the sidewash velocity induced normal to the tail leading edge at each spanwise station. Since the effects of image vortices must be considered and it is preferred that the circle theorem be used, the wake vortex circulation vector is resolved parallel to the body axis as before. In this case, however, instead of simply resolving Γ_s through some angle analogous to ξ, as was done for the body above, a new strength is defined which will produce the same values of sidewash velocity as did the original vortex. A single vortex in the wake plus its images will induce some distribution of sidewash velocity v along the tail leading edge. The average value of this sidewash is

$$\frac{1}{p}\int_a^p v\,dz$$

If now the average sidewash is divided by the axial velocity $V\cos\alpha$, the average angle of attack induced on the tail is obtained. Using the result from slender body theory, that for low aspect ratio tails typical of missile configurations the slope of normal force coefficient is given by $\pi AR/2$, the normal force coefficient induced on the tail due to the ith vortex may be expressed formally as

$$C_{N_i}=\frac{\pi AR\,A_T}{2pV\cos\alpha A_B}\int_a^p v_i\,dz \quad (3)$$

In order to determine rolling moment induced on the missile due to the vertical tail, the resultant normal force is assumed to act at the centroid of the sidewash velocity distribution or, for the ith vortex

$$C_{\ell_i}=C_{N_i}\left\{a+\int_0^p v_i z\,dz\Big/\int_0^p v_i\,dz\right\}\frac{A_T}{A_B} \quad (4)$$

The total induced forces and moments are obtained by summing the effects of all vortices in the wake. Yawing moment

induced by the tail is calculated by assuming that the resultant loading is located at the midpoint of the leading edge.

The above procedure has been generalized to handle tails at any roll angle. In this way, the contributions of all tails to side forces and yawing and rolling moments may be determined.

Since arbitrary roll angles can be considered, this raises potential problems when a vortex core intersects the leading edge. For potential vortices of the kind used here, flow velocities become extremely high near the core, resulting in unrealistically high induced sidewash angles. This problem was circumvented by introducing into each vortex a solid core of radius 0.25 body radius.[18]

When the tail intersects this core, calculations are discontinued. If the core passes over a tail while angle of attack is increasing, the forces and moments are faired across the gap within which calculations are not performed. This procedure has proved quite satisfactory in practice.

Instead of the slender body theory approach to tail force, strip theory might have been employed. It was felt, however, that the former was more appropriate for the low aspect ratio tails for which the program would probably be used. The program is flexible enough, however, that strip theory could be easily introduced if it were considered necessary.

At this stage then, the effects of the wake vortices on bodies and tails are calculable. Comparisons will now be presented between predicted and experimental forces and moments to illustrate the performance of this engineering model. Bodies alone and with cruciform tails will be considered. The effect of varying the number of vortices considered will be shown.

Comparisons with Experiment

Program predictions have been compared against various experimental data generated on a selection of the Martin Marietta Aerodynamic Research Models.[16] The basic model used for high angle data generation was a 10-caliber tangent ogive/cylinder. This body was tested alone and with several sets of cruciform tails affixed. Each tail was individually instrumented so that program predictions of vertical tail forces and moments could be checked for "plus" attitudes. For tails other than vertical, the program would predict only the incremental force generated on them by the asymmetric wake. Freestream effects were not taken into account, and hence forces for nonvertical tails will not be discussed. However, since the differences between nonvertical tails due to asymmetric effects were presumed to be valid for "plus" and "cross" attitudes, the program was used to predict rolling moments for these attitudes.

The first comparison is shown in Fig. 9. Here, program predictions of normal force on a vertical lee side tail fixed to the body are compared against experimental data. Also shown is the effect of considering all of the vortices in the wake and of using only those vortices closest to the body, i.e., the growing vortices. It will be seen that the magnitude of tail force is predicted within a few per cent using only the growing vortices, while use of all vortices produces a significant discrepancy. The angle at which asymmetry begins is matched only fairly, but the angle at which the appearance of a new wake vortex drives the tail force in the opposite direction is matched within a few degrees. From this evidence, it is concluded that the growing vortices tend to dominate the tail aerodynamic characteristics. The second comparison is shown in Figs. 10a and b. Here, predictions of isolated body side force and yawing moments are compared against test data. Again, the effects of considering all of the wake vortices separately from the growing vortices are considered. To make the distinction clearer, no attenuation of nongrowing vortex effects has been included. It will be seen that use of all the vortices produces divergent results which have none of the oscillatory character typical of asymmetric effects and evidenced by the data. This is because the net wake circulation remains unchanged in sign, regardless of the number of vortices present. Use of the growing vortices only, on the other

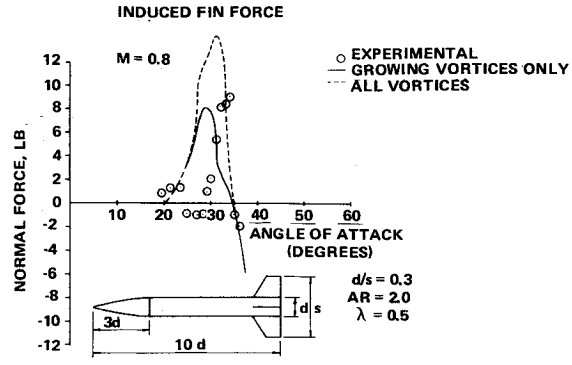

Fig. 9 Comparison between predicted and experimental vertical fin normal force.

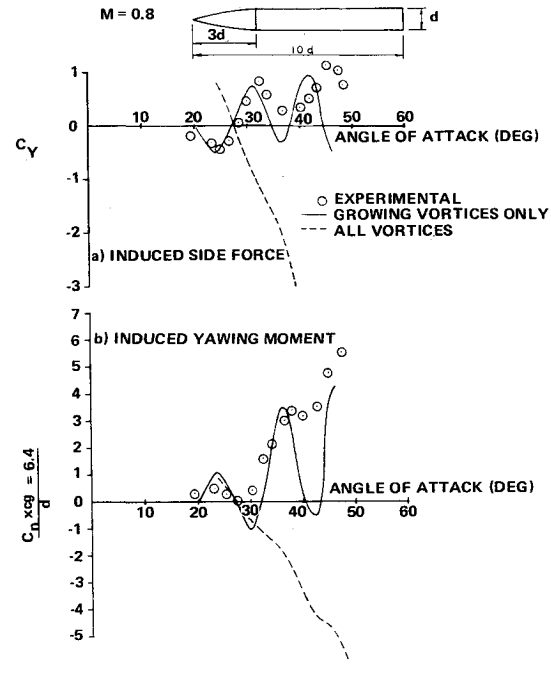

Fig. 10 Comparison between predicted and experimental results

hand, yields quite good matching of force and moment magnitudes, as well as angles of onset and new vortex appearance, at least until several vortices are present. While matching is not exact at the higher angles it is clear that use of the program will produce satisfactory preliminary design level estimates for isolated bodies.

Lastly, comparisons are shown between predictions and data for the 10-caliber body with a variety of tails. Based on the results for tails and bodies, these comparisons contain the effects of growing vortices only. Figs. 11a, b, and c show side force, yawing moment, and rolling moment comparisons, respectively. Prediction accuracy is generally satisfactory. In most cases the magnitudes of the quantities are predicted quite closely. On the other hand, the onset of asymmetry and the appearance of new vortices are not always so accurately reproduced.

In general, the model performs quite reasonably. In view of the changes in force and moment data magnitudes and signs which can be obtained by rotation of test models[1,3,4] some degree of fortuitousness might be assigned to the results shown. On the other hand, it is unlikely that any measured forces and moments will be significantly greater than those calculated, since the model contains all the essential elements of the vortex flowfield, both in magnitude and locations. In addition, it is felt that the means of calculating flowfield effects are adequately founded in theory.

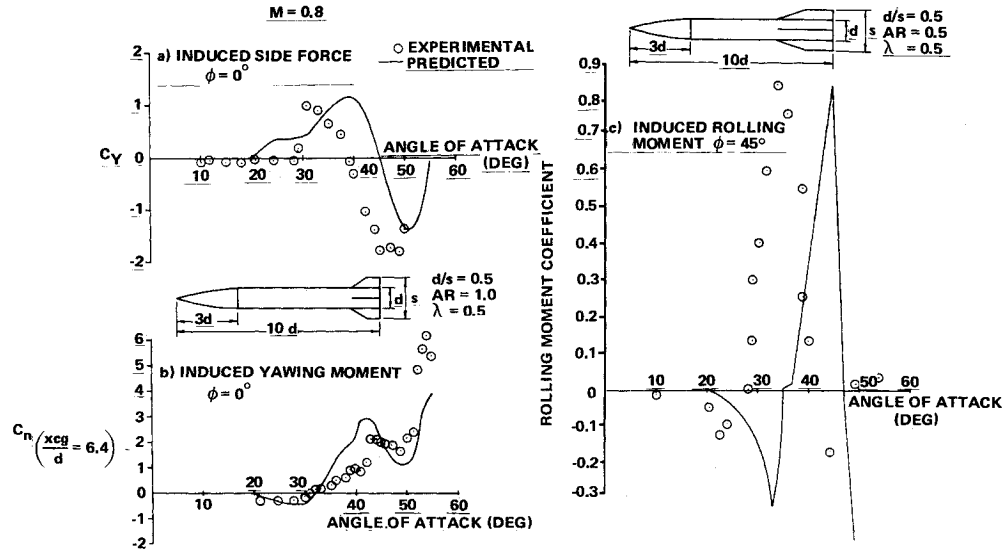

Fig. 11 Comparison between predicted and experimental results.

Conclusions

It has been shown that an engineering type model for estimating body wake asymmetric vortex effects can be straightforwardly constructed. The results indicate that the vortices growing in the vicinity of the body dominate the induced effects. This appears intuitively correct, particularly in the context of the two-dimensional analogy. There, the vortices closest to the body would be expected to produce the presure and velocity distributions which generate the forces and moments, with the remainder of the vortices having little effect as they pass downstream. It is not unexpected then, that the three-dimensional case should give similar results. However, although the street vortices have been shown to have relatively little impact, the experimental information on their strengths and shedding frequencies remains of central importance since it defines the bounds of growing vortex strength and shedding frequency. The model has been shown to yield generally satisfactory predictions and at this stage is considered a usable preliminary design tool.

References

[1] Thomson, K.D. and Morrison, D.F., "Spacing, Position, and Strength of Vortices in the Wake of Slender, Cylindrical Bodies at Large Incidence," *Journal of Fluid Mechanics,* Vol. 50., Dec. 1971, pp. 751-783.

[2] Thomson, K.D., "Estimation of the Drag of Circular Cylinders at Subcritical Reynolds Numbers and Subsonic Speeds," *Journal of Royal Aeronautical Society,* Vol. 74, Sept. 1970, pp. 762-763.

[3] Pick, G.S., "Investigation of Side Forces on Ogive-Cylinder Bodies at High Angles of Attack in the $M = 0.5$-1.1 Range," AIAA Paper 71-570, 1971, Palo Alto, Calif.

[4] Briggs, M.M., Clark, W.H., and Peoples, J.R., "Occurrence and Inhibition of Large Yawing Moments during High Incidence Flight of Slender Missile Configuration," AIAA Paper 72-968, 1972, Palo Alto, Calif.

[5] Fleeman, E.L. and Nelson, R.C., "Aerodynamic Forces and Moments on a Slender Body with a Jet Plume for Angles of Attack up to 180°," AIAA Paper 74-110, 1974, Washington, D.C.

[6] Fidler, J.E., "Approximate Method for Estimating Wake Vortex Strength," *AIAA Journal,* Vol. 12, May 1974, pp. 633-635.

[7] Kubin, J.F., "An Analysis of Steady Asymmetric Vortex Shedding from a Missile at High Angles of Attack," Thesis, USAF Institute of Technology, GAM/AE/73A-13, Wright-Patterson AFB, Ohio, Dec. 1973.

[8] Thomson, K.D., ,'Estimation of Viscous Normal Force, Pitching Moment, Side Force, and Yawing Moment on Bodies of Revolution at Incidences up to 90°," WRE Report-782, Australian Weapons Research Establishment, Salisbury, South Australia, 1972.

[9] Wardlaw, A.B., "Prediction of Yawing Force at High Angles of Attack," *AIAA Journal,* Vol. 12, Aug. 1974, pp. 1142-1144.

[10] Allen, H.J., and Perkins, E.W., "Characteristics of Flow over Inclined Bodies of Revolution," RM A50L07, 1951, NACA.

[11] Perkins, E.W., and Jorgensen, L.H., "Comparison of Experimental and Theoretical Normal Force Distributions (including Reynolds Number Effects) on an Ogive-Cylinder at Mach 1.98," TN 3716, 1956, NACA.

[12] Kelley, H.R., "Estimation of Normal-Force, Drag, and Pitching-Moment Coefficients for Blunt Based Bodies of Revolution at Large Angles of Attack," *Journal of Aeronautical Sciences,* Vol. 21, Aug. 1954, pp. 549-555.

[13] Hill, J.A.F., "A Nonlinear Theory of the Lift on Slender Bodies of Revolution," Proceedings, U.S. Navy Symposium on Aeroballistics, U.S. Naval Ordnance Test Station, Report 5338, 1954.

[14] Milne-Thomson, L.M., *Theoretical Hydrodynamics,* Third Ed., MacMillan, New York, 1955.

[15] Liepmann, H.W. and Roshko, A., *Elements of Gasdynamics,* Wiley, New York, 1966.

[16] Fidler, J.E., "A Systematic Experimental Approach to Upgrading Missile Aerodynamic Technology," Ninth U.S. Navy Symposium on Aeroballistics, 1972.

[17] Achenbach, E., "Distribution of Local Pressure and Skin Friction around a Circular Cylinder in Cross Flow up to $Re = 5 \times 10^6$," *Journal of Fluid Mechanics,* Vol. 34, Dec. 1968, pp. 625-639.

[18] Jorgensen, L.H., and Perkins, E.W., "Investigation of Some Wake Vortex Characteristics of an Inclined Ogive-Cylinder Body at Mach Number 2," Report 1371, 1958, NACA.